NASA TECHNICAL MEMORANDUM

NASA TM X-64940

FLUID MANIFOLD DESIGN FOR A SOLAR ENERGY STORAGE TANK

By W. R. Humphries, E. I. Griggs, and
H. C. Hewitt

June 1975

NASA

George C. Marshall Space Flight Center
Marshall Space Flight Center, Alabama

MSFC - Form 3190 (Rev June 1971)

TECHNICAL REPORT STANDARD TITLE PAGE

1. REPORT NO.	2. GOVERNMENT ACCESSION NO.	3. RECIPIENT'S CATALOG NO.
NASA TM X-64940		

4. TITLE AND SUBTITLE	5. REPORT DATE
Fluid Manifold Design for a Solar Energy Storage Tank	June 1975
	6. PERFORMING ORGANIZATION CODE
7. AUTHOR(S)	8. PERFORMING ORGANIZATION REPORT #
W.R. Humphries, E.I. Griggs*, H.C. Hewitt**	
9. PERFORMING ORGANIZATION NAME AND ADDRESS	10. WORK UNIT NO.
George C. Marshall Space Flight Center Marshall Space Flight Center, Alabama 35812	11. CONTRACT OR GRANT NO.
	13. TYPE OF REPORT & PERIOD COVERED
12. SPONSORING AGENCY NAME AND ADDRESS	Technical Memorandum
National Aeronautics and Space Administration Washington, D.C. 20546	14. SPONSORING AGENCY CODE

15. SUPPLEMENTARY NOTES

Prepared by Structures and Propulsion Laboratory, Science and Engineering

*Associate Professor, Department of Mechanical Engineering, Tennessee Technological University.

**Professor, Department of Mechanical Engineering, Tennessee Technological University.

16. ABSTRACT

A design technique for a fluid manifold for use in a solar energy storage tank is given. This analytical treatment generalizes the fluid equations pertinent to manifold design giving manifold pressures, velocities, and orifice pressure differentials in terms of appropriate fluid and manifold geometry parameters. Experimental results used to corroborate analytical predictions are presented. These data indicate that variations in discharge coefficients due to variations in orifices can cause deviations between analytical predictions and actual performance values.

17. KEY WORDS	18. DISTRIBUTION STATEMENT
	Unclassified – Unlimited W.R. Humphries

19. SECURITY CLASSIF. (of this report)	20. SECURITY CLASSIF. (of this page)	21. NO. OF PAGES	22. PRICE
Unclassified	Unclassified	21	NTIS

TABLE OF CONTENTS

LIST OF ILLUSTRATIONS

LIST OF TABLES

DEFINITION OF SYMBOLS

Symbol	Definition
A	manifold cross-sectional area, cm^2 ($in.^2$)
C_D	coefficient of discharge
D	inside diameter of pipe manifold, cm (in.)
d	diameter of hole, cm (in.)
f	friction factor
g_c	dimensional constant, 1×10^5 g-cm/N-s^2 (32.174 lbm-ft/lbf-s^2)
H	supply head, liquid level in supply reservoir measured above the outlet in the manifold, cm (in.)
i	integer denoting axial location of holes
k	total number of holes in the manifold
K′	1 when SI units are used and 144 when British units are used
K″	2 when SI units are used and 288 when British units are used
K‴	1 when SI units are used and 12 when British units are used
L	length between two points in the flow field, cm (in.)
m	integer denoting number of axial locations of holes
n	integer denoting number of holes at each axial location
P	static pressure, N/cm^2 absolute (psia)
V	average velocity within manifold, cm/s (ft/s)
w	mass flow rate, g/s (lbm/sec)
Δ	difference or increment
ρ	liquid density, g/cm^3 (lbm/ft^3)
μ	absolute viscosity, g/cm-s (lbm/ft-s)

DEFINITION OF SYMBOLS (Concluded)

Symbol	Definition
Subscripts	
e	environmental conditions external to manifold
i	denotes value just upstream of axial location i
j	summation index, integer
o	designates conditions for a hole
s	supply conditions
1,2	denotes two separated points along the flow field

TECHNICAL MEMORANDUM X-64940

FLUID MANIFOLD DESIGN FOR A SOLAR ENERGY STORAGE TANK

INTRODUCTION

In the design of a solar system in which a liquid medium is used for energy transport, the energy storage tank design is of paramount importance. For a system where either the collector or heater/air conditioner (HTR/AC) fluid loops flow into the tank, the designer must consider all fluid/thermal phenomena occurring within the tank. Two fluid phenomena which may be present in a system of this type are stratification and flow "short circuiting" or "channeling." The first phenomenon may be used to advantage by the designer, while the second phenomenon is normally avoided if possible. The first phenomenon is caused by a temperature gradient in the fluid from the tank top to the bottom of the tank, with the heavier cold fluid collecting in the bottom of the tank and the less dense high temperature fluid rising to the top. In a proper design this thermal condition may be used to advantage by supplying the solar collector fluid from colder fluid in the tank bottom and returning the outlet collector fluid to the tank top. The HTR/AC fluid loop may be supplied from the warm top and the cooler return fluid returned to the tank bottom. This arrangement tends to promote stratification thereby improving collector efficiency and minimizing supplementary energy utilization.

Evidence of the second phenomenon is seen by the flow of fluid within the tank from the collector and/or HTR/AC return to the inlet, forming a channel within the tank. This phenomenon, if it occurs, has the adverse effect of supplying warmer fluid to the collector and cooler fluid to the HTR/AC loop components. One technique used to avoid this undesirable occurrence is by manifolding the return line. This distributes the return fluid over a larger zone, decreasing the fluid stream velocity and thereby lessening the tendency to channel.

In early tests of the Marshall Space Flight Center (MSFC) solar house, channeling and stratification were observed in the energy storage tank. Channeling predominately occurred within the tank between the HTR/AC loop outlet and inlet. This prevented use of the warmer stagnate fluid bulk. As a result, a manifold was designed to be submersed in the energy storage tank on the HTR/AC return line. The manifold was located in the tank bottom to promote the stratification already present in the tank.

Some considerations relative to the design of such a manifold are presented in this report. Some attention is given to the principles useful in making design predictions, and this is followed by the presentation and discussion of some related experimental results.

The application of interest is schematically illustrated in Figure 1.

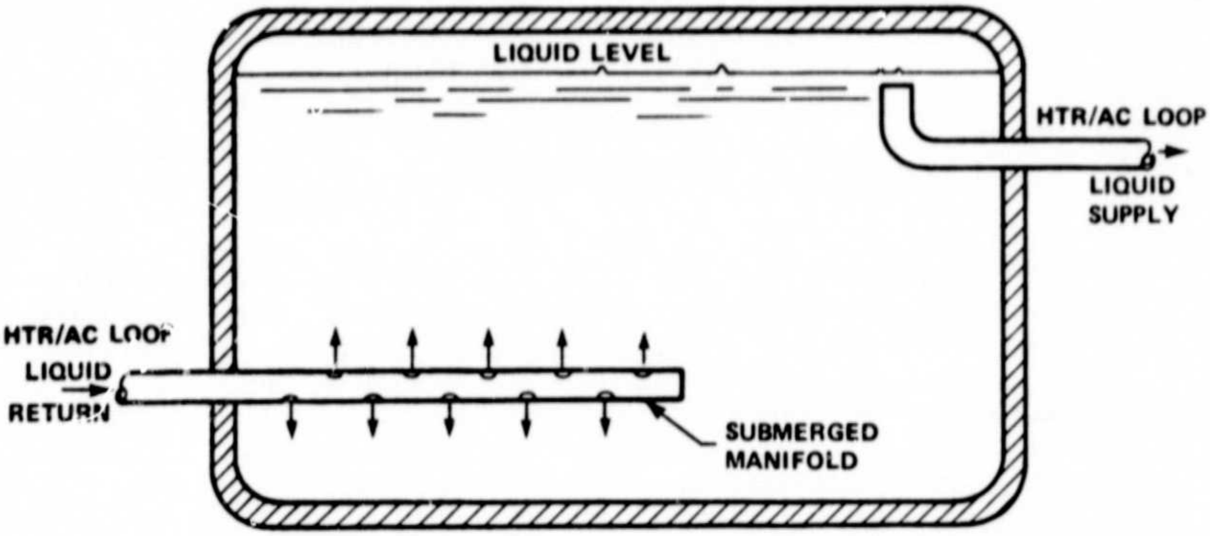

Figure 1. Schematic of liquid return manifold in an energy storage vessel.

FUNDAMENTAL CONSIDERATIONS

When a liquid flows through a passage of constant cross-sectional area, there is a drop in static pressure due to viscous effects. Even when viscous effects are negligible, a significant drop in static pressure can be produced by reducing the flow area as is done with a nozzle. Conversely, an increase in static pressure occurs if there is an increase in area as in the case of a diffuser. When flow occurs through a constant area passage with bleed off at the walls, the fluid extraction reduces the average velocity in the passage; a related increase in static pressure is associated with this reduction in average velocity. Consequently, flow within a manifold of constant cross-sectional area having openings in the walls for distribution of the discharge will experience a reduction in static pressure due to viscous effects and an increase due to the velocity decrease. The resultant static pressure variation will depend on the relative importance of these two factors. The maximum increase in static pressure due to the decrease in velocity is given by the dynamic head of the flow. In equation form, the increase in pressure from point 1 in the flow to another point 2 downstream of the first is given by

$$ {}_1\Delta P_2 = \rho \frac{(V_1{}^2 - V_2{}^2)}{2g_c} - f\left(\frac{L}{D}\right) \rho \frac{V_2{}^2}{2g_c} \qquad (1) $$

where V_1 is the average velocity upstream of point 1 and V_2 is the average velocity of the flow between points 1 and 2.

As a specific example, suppose it is desired to drill a number of holes in a straight segment of pipe to serve as a manifold such that the flow of liquid delivered from each hole is the same. A schematic of the arrangement is shown in Figure 2. The static pressure at station $i + 1$ (Fig. 2) can be expressed by

$$P_{i+1} = P_i + \rho \frac{(V_i^2 - V_{i+1}^2)}{K'' g_c} - \frac{(fL)_{i+1} V_{i+1}^2}{D K'' g_c} \quad . \tag{2}$$

For equal flow from each hole, the flow rate discharged through a hole is w/k and the flow rate discharged at each axial location of holes is nw/k. The flow rate within the manifold just upstream of axial location i is

$$w_s \left[1 - \frac{(i-1)n}{k} \right] \quad . \tag{3}$$

The velocities V_i and V_{i+1} are then given by

$$V_i = \frac{w_s}{\rho A} \left[1 - (i-1) \frac{n}{k} \right] K' \tag{4}$$

and

$$V_{i+1} = \frac{w_s}{\rho A} \left[1 - \frac{in}{k} \right] K' \quad . \tag{5}$$

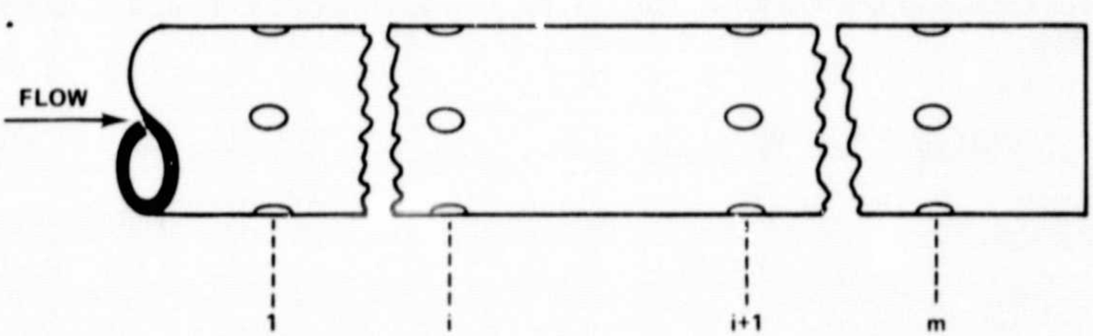

Figure 2. Schematic of flow manifold.

Then, it follows that

$$V_i^2 - V_{i+1}^2 = \left(\frac{K' \; w_s \; n}{\rho A k}\right)^2 \left(1 + 2\frac{k}{n} - 2i\right) \quad . \tag{6}$$

Insertion of equations (5) and (6) into equation (2), after some rearrangement, yields

$$P_{i+1} = P_i + \left(\frac{K' \; w_s \; n}{\rho A k}\right)^2 \frac{\rho}{K'' g_c} \left[\left(1 + 2\frac{k}{n} - 2i\right) - \left(\frac{fL}{D}\right)_{i+1} \left(i - \frac{k}{n}\right)^2\right] \quad . \tag{7}$$

Equation (7) relates the pressure at two adjacent axial stations. The pressure at location i can also be related to the supply pressure by

$$P_i = P_s - \frac{K' \; w_s^2}{2 g_c \rho A^2} \left\{\left(\frac{fL}{D}\right)_1 - \sum_{j=1}^{i-1} \left(\frac{n^2}{k^2}\right) \left(1 + 2\frac{k}{n} - 2j\right) - \left(\frac{fL}{D}\right)_{j+1} \left(j - \frac{k}{n}\right)^2 \Big]\right\} \quad . \tag{8}$$

The flow rate through an orifice can be expressed by

$$w_o = C_D \frac{A_o}{K'''} \sqrt{2 g_c \rho (\Delta P)_o} \quad . \tag{9}$$

For a particular hole located at station i, the pressure difference to be used in equation (9) is

$$(\Delta P_o)_i = P_i - P_e \quad . \tag{10}$$

In summary, when the objective is to design a manifold that delivers equal flow from each hole, equation (8) can be used to predict the pressure at i and equations (9) and (10) can be used to predict the required opening size. More generally, equations (2), (9), and (10) can be used for predictions with other than equal flow requirements.

It should be emphasized, however, that there are two factors of considerable uncertainty when employing the preceding principles for design predictions. The first is associated with the coefficient of discharge, C_D, which is used in equation (9) and the second is related to the friction factor, f, to be used in equation (2) or equation (8).

EXPERIMENTAL STUDY

A test arrangement was set up to facilitate investigation of the discharge of water from holes drilled in a straight segment of pipe or tubing. Figure 3 schematically illustrates the arrangement. Water was supplied to the manifold through an opening near the bottom of a metal reservoir. A quick opening valve located at the inlet to the manifold allowed starting and stopping of the flow. Two openings located at two different levels in the side of the reservoir served as overflow outlets. These allowed an approximately constant head to be impressed on the manifold inlet during all tests. Two different levels were possible depending on which overflow opening was blocked. The water which drained through the overflow together with any make-up water was collected in a secondary reservoir. A pump was used to circulate the flow from the secondary reservoir back to the primary reservoir.

Tests were initiated by opening the quick-acting valve and establishing flow through the manifold. Air bleeds were used to eliminate any trapped air from within the manifold. The pump was throttled until the liquid level in the tank settled at a constant value. Even though attempts were made to maintain the same level for comparable tests, some slight variation existed simply because of limited resolution on the control of the return flow. After all conditions stabilized, a four liter (≈ 1 gallon) container was quickly inserted under each hole in the manifold. Subsequently, these were quickly removed and the collection time was measured and recorded using a stop watch. The weight of water collected was measured. The containers were dried with paper towels and prepared for subsequent tests. During the tests the level of water in the primary reservoir was monitored and measured.

Three separate manifolds were tested. The first two were made from straight pieces of 2.54 cm (1 in.) nominal Schedule 40 steel pipe [2.664 cm (1.049 in.) I.D.]. The third was made from a straight piece of 2.54 cm (1 in.) O.D. by 1.91 cm (0.75 in.) I.D. plexiglas tubing. In all cases, the manifolds were rigidly mounted and leveled on the table of a milling machine. The center of the pipe was located by means of a dial indicator. The holes were then drilled with the milling machine. Tests performed on each manifold and the corresponding results are outlined in the following paragraphs.

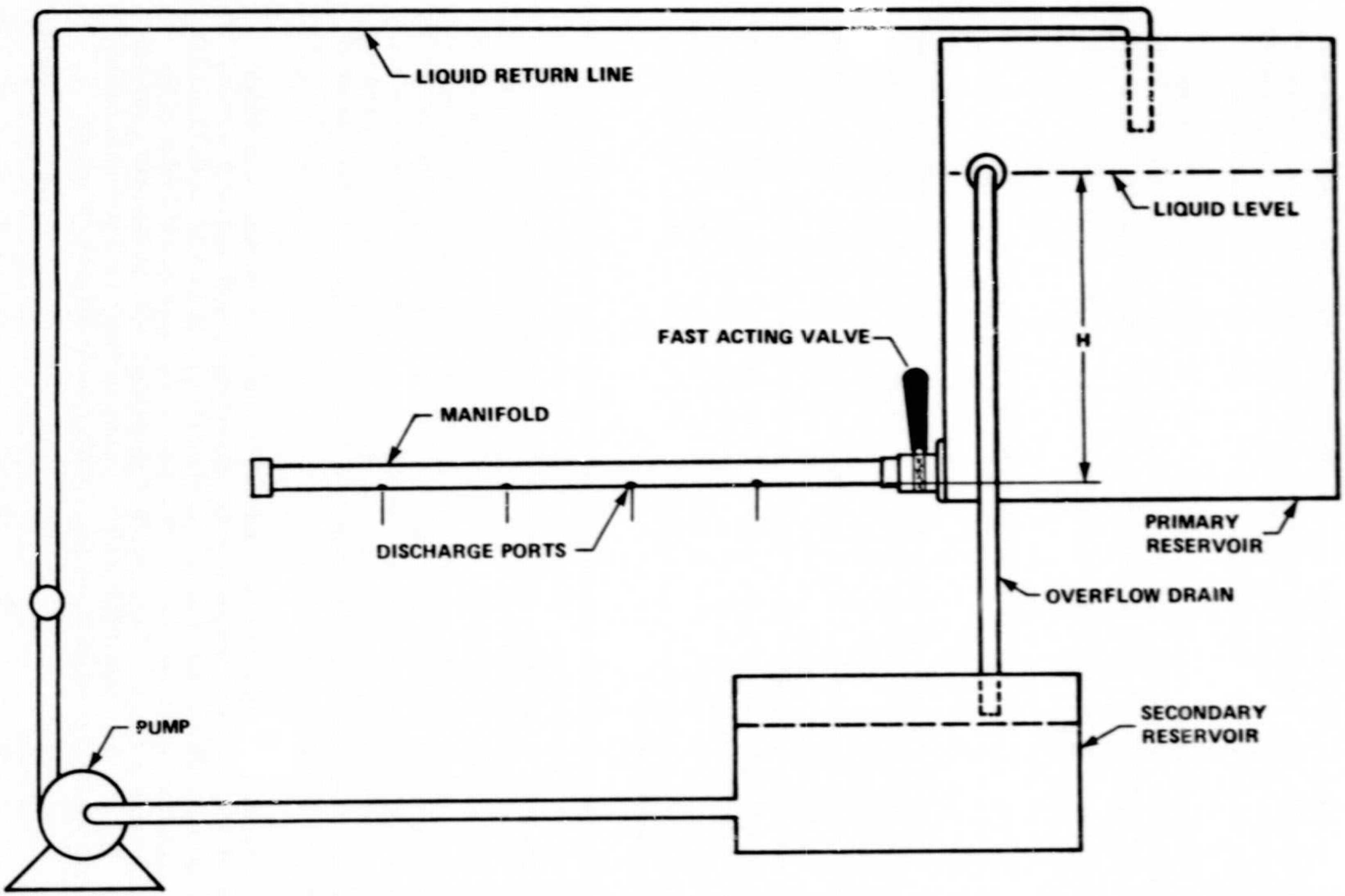

Figure 3. Schematic of experimental apparatus for conducting manifold tests.

In the first arrangement, three holes were drilled on 15.2 cm (6 in.) centers with a 0.511 cm (0.201 in.) diameter drill bit. The location of these in relation to the flow inlet is shown in Figure 4. The other end of the manifold was capped. The manifold was oriented so that the discharge from each hole would be vertically downward. Directly opposite each discharge hole, another hole was drilled and an adaptor was soldered on the pipe which permitted attachment of a vertical section of glass tubing above the hole. These were incorporated to provide an indication of the static pressure at each discharge location. They were used to also bleed air out of this arrangement.

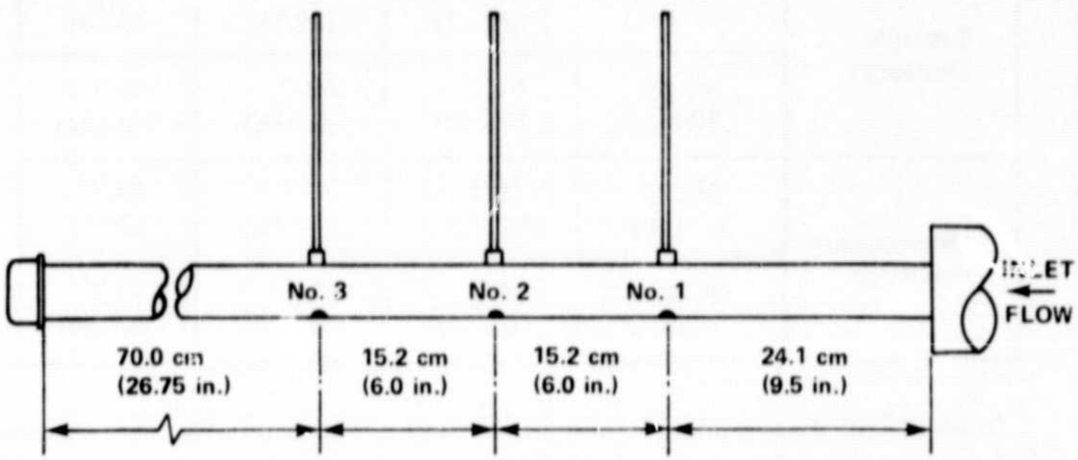

Figure 4. First test manifold with three 0.511 cm (0.201 in.) diameter holes.

Tests were performed with each hole separately opened and with all three open simultaneously. The data are shown in Table 1. In every case, the flow rates represent the average of at least five runs. Values of liquid level H were measured to within ±0.64 cm (1/4 in.). The data in Table 1 indicate that the flow rates decrease in the downstream direction for both cases with there being almost negligible difference between the results for simultaneous discharge and those for separate discharge. For separate discharge, the percentage difference in the measured discharge rate, based on the high value, is 16.2 percent and the corresponding difference for simultaneous discharge is 20 percent. The percentage variation in the supply head for the case of separate discharge, again based on the high value, is only 2.5 percent. It should be noted that a 1 percent change in the pressure difference across an orifice should affect the flow rate by approximately 0.5 percent. Consideration of these data suggests that the differences in the measured flow rates must be due to differences in the configurations of the holes and, consequently, the associated discharge coefficients. The velocity decrease effect is not apparent in the data for simultaneous discharge. This is understandable because the largest dynamic head within the manifold occurs upstream of the first hole and for these data is approximately 0.5 cm (0.2 in.) of water which is less than 1 percent of the supply head. This considered together with the lengths involved and a reasonable estimate of a friction factor also indicates no noticeable frictional effects.

TABLE 1. TEST DATA FOR FIRST MANIFOLD WITH THREE 0.511 cm (0.201 in.) DIAMETER HOLES

		Hole Number		
		1	2	3
Separate Discharge	H, cm (in.)	76.8 (30.25)	74.9 (29.5)	76.2 (30.0)
	w, g/s (lbm/s)	67.2 (0.148)	62.7 (0.138)	56.3 (0.124)
Simultaneous Discharge	H, cm (in.)	74.9 (29.5)	74.9 (29.5)	74.9 (29.5)
	w, g/s (lbm/s)	68.1 (0.150)	62.2 (0.137)	54.5 (0.120)

In an attempt to alleviate discrepancies in the hole characteristics, each was reamed to 0.518 cm (0.204 in.) diameter, and an effort was made to scrape burrs off the inside edge of the holes. The tests were then repeated and the results are tabulated in Table 2.

The data shown in Table 2 do not follow an anticipated pattern. The 10 percent variation in discharge rate for the case of separate discharge and the 14 percent in the case of simultaneous discharge are not accounted for by the small differences in supply head. Differences in discharge coefficients must be the primary contributing factor.

TABLE 2. TEST DATA FOR FIRST MANIFOLD WITH THREE 0.518 cm (0.204 in.) DIAMETER HOLES

		Hole Number		
		1	2	3
Separate Discharge	H, cm (in.)	76.2 (30.0)	74.9 (29.5)	75.9 (29.875)
	w, g/s (lbm/s)	64.5 (0.142)	71.7 (0.158)	67.6 (0.149)
Simultaneous Discharge	H, cm (in.)	74.6 (29.375)	74.6 (29.375)	74.6 (29.375)
	w, g/s (lbm/s)	61.7 (0.136)	71.7 (0.158)	66.7 (0.147)

The second manifold was also made from a piece of 2.5 cm (1 in.) nominal diameter schedule 40 steel pipe [2.664 cm 1.049 in.) I.D.]. Six discharge holes were drilled using a 0.511 cm (0.201 in.) diameter bit. A different procedure for drilling the discharge holes was used. It was reasoned that, in the case of the first manifold, burrs might be present around the flow entrance of the discharge hole due to the fact that the drill bit emerged on that side as it came through from the outside. So, in the case of the second manifold, the holes were drilled completely through the manifold so that on one side the hole would be drilled with the bit entering the metal from the inside. These holes were then used as the discharge ports. The opposing holes were blocked with putty and tape. The location of the holes are shown in Figure 5.

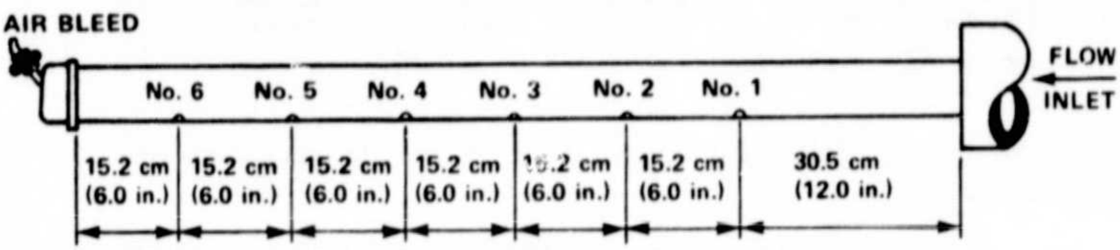

Figure 5. Second test manifold with six 0.511 cm (0.201 in.) diameter holes.

For this second test manifold, no measurements of separate discharge were made. Seven runs of simultaneous discharge were made with a supply head of approximately 76 cm (30 in.) of water. The averaged flow rates are tabulated in Table 3. The maximum difference in measured flow rate, based on the highest value, is 2.5 percent. The dynamic head upstream of the first hole is 1.68 cm (0.66 in.) of water. Therefore, an upper bound for the velocity decrease effect on the flow discharge would be less than 1 percent. Also, using a friction factor of 0.02, an upper bound for viscous effects would also be less than 1 percent. Since these two influences, as discussed earlier, are counteracting and small for this case, one would not expect to detect any noticeable influence. Since the measured flow rates are very close, it is concluded that this method of drilling discharge holes provides more consistent coefficients of discharge.

TABLE 3. TEST DATA FOR SECOND MANIFOLD WITH SIX 0.511 cm (0.201 in.) DIAMETER HOLES, 76 cm (30 in.) OF WATER SUPPLY HEAD AND SIMULTANEOUS DISCHARGE

	Hole Number					
	1	2	3	4	5	6
w, g/s (lbm/s)	53.1 (0.117)	54.0 (0.119)	52.7 (0.116)	53.6 (0.118)	53.1 (0.117)	53.6 (0.118)

The third manifold was made from a piece of 2.5 cm (1 in.) O.D. by 1.9 cm (0.75 in.) I.D. plexiglas tubing. Hole locations are shown in Figure 6. A series of tests encompassing separate and simultaneous discharge were made with four 0.485 cm (0.191 in.) diameter holes. Subsequently, another series of tests were conducted with the holes enlarged to 0.635 cm (0.250 in.) diameter. The results are tabulated in Tables 4 and 5.

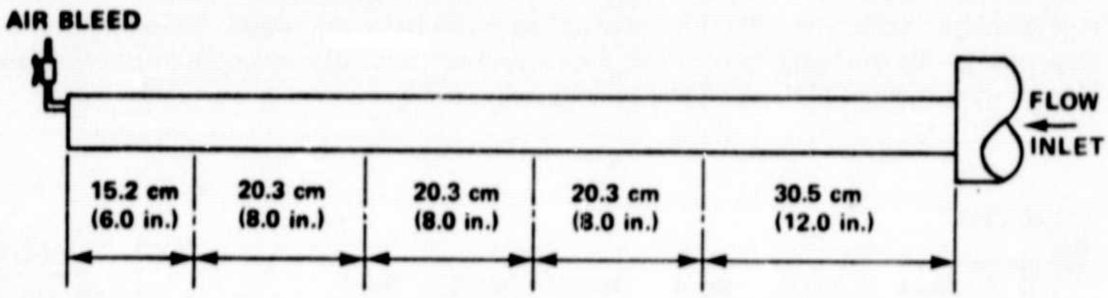

Figure 6. Third manifold made from 2.5 cm (1 in.) plexiglas tubing.

TABLE 4. TEST DATA FOR THIRD MANIFOLD WITH FOUR 0.485 cm (0.191 in.) DIAMETER HOLES

		Hole Number			
		1	2	3	4
Separate Discharge	H, cm (in.)	42.5 (16.75)	42.5 (16.75)	42.5 (16.75)	42.5 (16.75)
	w, g/s (lbm/s)	41.0 (0.0903)	42.9 (0.0945)	42.8 (0.0942)	43.6 (0.0955)
Simultaneous Discharge	w, g/s (lbm/s)	37.2 (0.0819)	39.0 (0.0860)	40.1 (0.0883)	41.6 (0.0917)
Separate Discharge	H, cm (in.)	76.8 (30.25)	76.8 (30.25)	76.8 (30.25)	76.8 (30.25)
	w, g/s (lbm/s)	54.9 (0.121)	56.8 (0.125)	55.8 (0.123)	57.2 (0.126)
Simultaneous Discharge	w, g/s (lbm/s)	50.4 (0.111)	57.8 (0.114)	54.0 (0.119)	56.3 (0.124)

TABLE 5. TEST DATA FOR THIRD MANIFOLD WITH FOUR 0.635 cm (0.250 in.) DIAMETER HOLES

		Hole Number			
		1	2	3	4
Separate Discharge	H, cm (in.)	43.8 (17.25)	43.8 (17.25)	43.8 (17.25)	43.8 (17.25)
	w, g/s (lbm/s)	73.5 (0.162)	74.9 (0.165)	73.1 (0.161)	71.7 (0.158)
Simultaneous Discharge	w, g/s (lbm/s)	59.9 (0.132)	62.2 (0.137)	63.6 (0.140)	66.7 (0.147)
Separate Discharge	H, cm (in.)	76.8 (30.25)	76.8 (30.25)	76.8 (30.25)	76.8 (30.25)
	w, g/s (lbm/s)	94.4 (0.208)	97.6 (0.215)	91.7 (0.202)	91.7 (0.202)
Simultaneous Discharge	w, g/s (lbm/s)	81.7 (0.180)	83.5 (0.184)	84.9 (0.187)	87.6 (0.193)

Consideration of the differences in separate discharge rates of approximately 5 percent and the pattern of the differences suggest that the differences must be attributable to variations in the coefficients of discharge. In all four cases involving simultaneous discharge, the rate increases sequentially downstream, a pattern expected if the velocity decrease effect is larger than the viscous effect and there are no drastic variations in the discharge coefficients.

CONCLUSION

The design of a manifold can be approached using the basic principles outlined, and the distribution pattern is definitely dependent on the relative magnitudes of the viscous and velocity decrease effects. Uncertainty in discharge coefficients and applicable friction factors renders precise design predictions somewhat questionable. Based on the experimental work done here, the method of drilling holes could have more influence on the discharge coefficient than slight variation in diameter. Consequently, care should be exercised in drilling holes in a pipe to serve as a manifold to achieve reasonable uniformity in discharge coefficients. If the objective is to drill a number of holes to supply equal discharge, this can be achieved by sizing the holes such that the pressure drop across an individual hole is much larger than either the velocity decrease or viscous values. This may not be possible, however, if the total pressure drop across the manifold is to be kept at a minimal value. In such a case, the equality of discharge probably cannot be estimated with a closer degree of certainty than that associated with the discharge coefficients.

A manifold has been installed in the MSFC solar house energy storage tank which was designed using the design techniques given herein. This manifold is installed in the HTR/AC fluid loop and situated in the tank bottom. Preliminary data indicate that the manifold is surpressing "short circuiting" while maintaining a maximum amount of fluid stratification.

APPROVAL

FLUID MANIFOLD DESIGN FOR A SOLAR ENERGY STORAGE TANK

By W. R. Humphries, E. I. Griggs, and H. C. Hewitt

The information in this report has been reviewed for security classification. Review of any information concerning Department of Defense or Atomic Energy Commission programs has been made by the MSFC Security Classification Officer. This report, in its entirety, has been determined to be unclassified.

This document has also been reviewed and approved for technical accuracy.

J. WAYNE LITTLES
Chief, Life Support and Environmental Branch

GEORGE D. HOPSON
Chief, Engineering Analysis Division

ALEXANDER A. McCOOL
Director, Structures and Propulsion Laboratory